Centre for Research on Settlements and Urbanism

Journal of Settlements and Spatial Planning

Journal homepage: https://jssp.reviste.ubbcluj.ro

A New Approach for Identification and Analysis of Urban Heat Island Hotspots

Zsolt MAGYARI-SÁSKA[1], Csaba HORVÁTH*[2], Sorin POP[3], Adina-Eliza CROITORU[2]

** Corresponding author*

[1] Babeş-Bolyai University, Faculty of Geography, Department of Extensions, Gheorgheni Branch, Cluj-Napoca, ROMANIA

[2] Babeş-Bolyai University, Faculty of Geography, Department of Physical and Technical Geography, Research Centre for Sustainable Development, Cluj-Napoca, ROMANIA

[3] Creative Space SRL, Baia Mare, ROMANIA

✉ zsolt.magyari@ubbcluj.ro 0000-0002-5572-4132

✉ csaba.horvath@ubbcluj.ro 0000-0002-5691-2485

✉ sorin@cspace.ro 0009-0006-0858-6765

✉ adina.croitoru@ubbcluj.ro 0000-0003-1235-4327

DOI: https://doi.org/10.24193/JSSP.2024.2.01

Received: 01 July 2024

Received in revised form: 06 November 2024

Accepted for publication: 25 November 2024

Available online: 05 December 2024

K e y w o r d s: *urban heat island, hotspots severity detection, R data analysis, GIS, Landsat thermal band*

A B S T R A C T

Cities are heating up faster than their rural counterparts due to the urban heat island phenomenon, with severe heat accumulation in various areas – hotspots. This study proposes a new approach to analysing urban heat islands by detecting and hierarchising their associated hotspots based on their severity derived from the combination of intensity and frequency. The new method, implemented in R, uses Landsat thermal band data, study area boundaries, and an imperviousness layer to pinpoint critical areas. It consists of a three-step process: i. identifying and prioritising hotspots for each usable satellite image; ii. computing the intensity and frequency, and iii. calculating severity and generating the maps. Combining reclassified multi-image intensity and persistence data, we derived nine classes representing the range from the most frequent and intense areas to the least. Incorporating the imperviousness layer, the hotspot extension is dramatically reduced. The resulting hotspot maps provide valuable insights for urban planners and policymakers, highlighting the most vulnerable regions within the urban area and signalling the need for targeted administrative interventions. This comprehensive analysis was also applied to cold spots, ensuring a thorough understanding of the most and least critical regions.

1. INTRODUCTION

Urban areas are increasingly experiencing the adverse effects of the urban heat island (UHI) phenomenon, which amplifies the effects of global warming and climate change (Gartland, 2012). The concept of UHIs, as detailed by Santamouris (2020), highlights their emergence as a direct response to urban development and the concentration of heat-absorbing surfaces in cities. While Atmospheric Urban Heat Island (AUHI) is difficult to assess without an in-place urban climate monitoring system, remote sensing data proved to be very useful in retrieving land surface temperature (LST). Surface Urban Heat Island (SUHI) is detected based on LST differences between urban and rural areas (Voogt and Oke, 2003). Thus, remote sensing technology has brought a new viewpoint to understanding UHI in large areas, making regional or global studies more efficient and less expensive (Sanyal and Lu, 2004; Zhou et al., 2015; Zhou et al., 2022). Having the advantages of an extensive detection range and comprehensive space information, the SUHI has been largely used worldwide to investigate urban thermal features and their associated urban heat island effects (Cui et al., 2021; Derdouri et al., 2021; Hu and Brunsell, 2013; Zhou et al., 2022).

Based on an extensive literature review analysis, Wang and Chang (2020) found that, in relevant discussions, the term "hotspots" (HS) associated with the UHI (UHI-HSs) is not commonly mentioned, and the general perception of this term refers to the areas with the highest temperature or heat-related risks, but there is no consensus on their definition, or how their thresholds or indicators should be chosen. Many studies defined UHI-HSs as only an ambiguous description of high-temperature areas (Ho et al., 2016; Ketterer and Matzarakis, 2016; Silva et al., 2018), whereas others indicated that there is a significant threshold for the impact of heat on human health, and, once exceeded, the risk of mortality will become increasingly sensitive to slight changes in temperature (Houghton et al., 2012). However, since there are certain limitations in assessing the impact of heat on human health and there is not enough evidence to support this information, practitioners should find a way to establish a reasonable threshold range according to different spatial scales and objectives (Wang and Chang, 2020). Thus, detecting and analysing UHI-HSs is paramount for urban planning, public health, and environmental management.

Various methods have been developed and employed to identify UHI-HSs based on LST derived from satellite imagery, in-situ measurements or exploring thermal clusters through HS analysis tools. However, in-depth review research conducted by Wang and Chang (2020) indicated that only 2.5% of the studies involved persuasive methods to establish thresholds precisely and reasonably, and 28.75% of them presented a clear set of thresholds or referred to the definitions in previous studies, focusing on the concept and its meaning. The great majority did not provide a definition/method for UHI-HS identification, and they were merely considered common sense; extreme anomalies were often obscure in the temperature maps (37 %) or adopted subjective thresholds for easy operation and description (31.25%) (Wang and Chang, 2020).

Most studies considered satellite-based estimates of LST as being effective in explaining surface UHI (SUHI) effects since they provide relatively fast and low-cost information (Deilami et al., 2018). The multitude of approaches aiming to identify/detect the SUHI-HSs based on LST can be synthesised into the following typology: (i) using Jenk's natural discontinuity grading method, the highest area is considered an HS (Silva et al., 2018; Yin et al., 2018); (ii) classification of LST into a various number of classes, and the areas in the highest values are called HSs (Zhao et al., 2010; Sing Wong et al., 2016); (iii) exceeding a fixed or relative threshold above the urban area mean value (Martin et al., 2015; Mathew et al., 2016; Guha, 2017); (iv) a defined temperature fixed threshold to be exceeded combined with other features (area extension or distance to green areas) (Echevarria Icaza et al., 2017).

One of the most common tools for HS analysis in recent years is spatial autocorrelation clustering, which measures how a feature in one area relates to its surroundings. The main algorithms used are Getis-Ord Gi (a regional tool) (Abera and Yeshitela, 2024; Guerri et al., 2021b; Qiao et al., 2023) and Local Moran's I (a global tool) (Krellenberg et al., 2014; Abougendia, 2023). The Getis-Ord Gi statistic remains the most popular and largely used method for SUHI-HS detection, despite existing research that has explored the possibility of improving it (Bruns and Simko, 2017) or finding alternative approaches, such as employing LST curvature at various locations to delineate HS boundaries using the Multi-Scale Shape Index (Wang et al., 2015) or considering the fractal scale index by applying a percentile-based islet detection method for HS identification, with the top portion of the 3D temperature surface cut at a threshold value identified as UHI-HS (Shreevastava et al., 2019).

The present paper's main aim is to present a new method for analysing SUHI and, more specifically, to rank and detect SUHI-HSs severity inside the SUHI based on their intensity and frequency by using LST derived from Landsat imagery. This approach could become very useful for practical purposes, especially for territorial/urban planners in the process of prioritising interventions for reducing the UHI effect, since it is able to rank the severity of the HSs in a dedicated area. Additionally, it could answer questions such as: Which is/are the most critical area(s) in this city that need interventions to increase the thermal comfort in the city, taking into account the SUHI perspective? How extended is it/are they? How can it/they be identified considering both frequency and intensity?

2. THEORY AND METHODOLOGY

This section presents general information on the newly developed method. In our research, we propose and apply a new HS identification method, which is more effective compared to the largely used GetisOrd-Gi* methodology or with its enhanced version (Bruns and Simko, 2017). This innovative method, implemented in R, will be useful for urban planning decision-makers as it could support prioritising active interventions in specific areas, thus contributing to more efficient urban planning and public health strategies. To address the limitation imposed by the low spatial resolution of satellite thermal imagery commonly used (MODIS) (Wang and Chang, 2020), we employed images with a considerably improved spatial resolution (30 m), collected by Landsat missions and freely provided by the United States Geological Survey (U.S. Geological Survey [USGS], 2023).

The novelty of the proposed method consists of a few issues, making it more useful and reliable for end-users and enhancing its practicality for urban planners. Thus, it allows:

- ranking the SUHI-HSs based on their intensity at the entire considered area scale;

- flexible intensity thresholds (percentile-based) for SUHI-HSs identification;

- flexible number of SUHI-HSs identified based on their intensity;

- taking into consideration the inclusion or exclusion of imperviousness data for SUHI-HSs identification;

- assessment of the SUHI-HS severity accounting for their persistence and overall intensity calculated based on multiple images.

While the user can choose both intensity thresholds and the number of HSs to be identified, the proposed method allows SUHI-HSs to be delimited and uniquely identified. Unlike the classic Getis-Ord Gi* method, which indicates statistically significant value differences within a study area but does not connect adjacent values to form a connected surface, the new proposed method achieves this connectivity. Thus, it identifies and delimits SUHI-HSs as separate areas, starting from the current highest value and expanding the search in different directions in the geographical space (latitude/longitude).

This new approach of the territorial delimitation of SUHI-HSs applied to multiple satellite images of the same area provides the opportunity to examine their temporal persistence and intensity, as described in section 3.2. The implementation of the new method has been adapted for raster layers in R to increase accessibility to a broader audience. It considers the Landsat thermal band for LST detection and the limits of the study area as base input values, whereas the use of the imperviousness layer, as derived from the Sentinel-2 sensor of the European Space Agency (European Environment Agency, 2020), was set as an optional parameter. The method has several specific configurable parameters, as shown in the general framework A first pre-processing step is necessary to extract the study region from a larger area based on a mask vector layer. The second one consists of deciding whether or not the imperviousness will be considered. If included in the analysis, the SUHI-HSs identification will consider only the built-up/sealed areas, generating a higher fragmentation and a decrease in the SUHI-HS area. When detecting SUHI-HSs solely in built-up areas, the process consists of reclassifying the imperviousness raster layer, followed by cropping the imperviousness and LST layers to the desired study area and extracting the vegetation-covered zones from the LST using the reclassified binary imperviousness (Fig. 1).

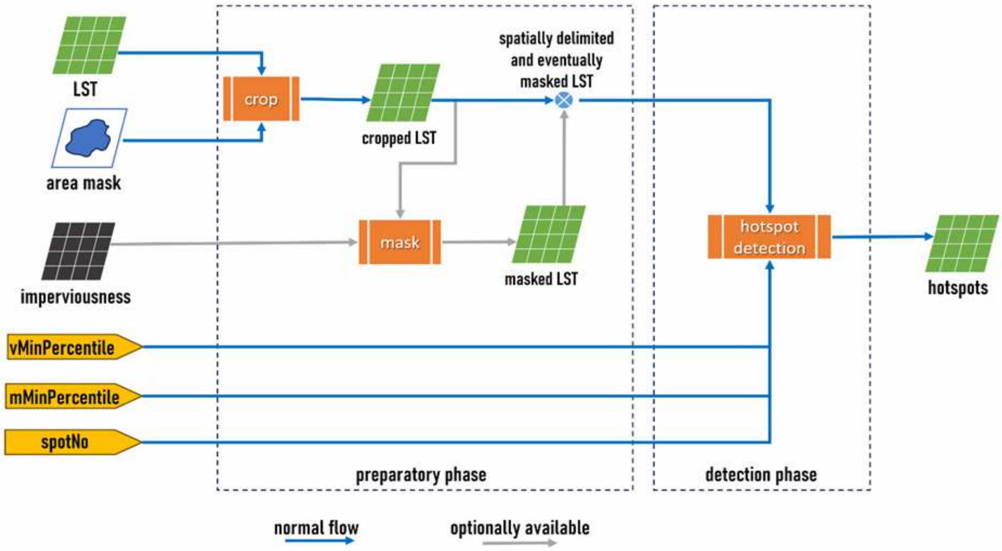

Fig. 1. SUHI-HS identification framework.

The full analysis method involves three steps:

(i) SUHI-HSs are identified and ranked for each usable satellite image (Croitoru et al., 2024);

(ii) The algorithm computes the SUHI-HSs persistence and the overall intensity, generating synthesis maps from all available images;

(iii) Persistence and overall intensity maps are used to derive the SUHI-HSs severity map.

All detection algorithms are presented in detail in the section *Results and Discussions*. The R code with functions used is freely available at: https://github.com/zsmagyari/SUHI. Beyond the HSs, the algorithms can be very easily adapted to detect cool spots (CSs).

3. RESULTS AND DISCUSSION

This section presents the algorithms for obtaining the SUHI-HSs and their associated parameters, while also comparing them, where possible, to the results obtained by applying the Getis-Ord Gi* method, already implemented in ArcGIS and consequently largely used.

3.1. SUHI-HSs detection algorithm based on single satellite images

The proposed method is a step-by-step identifying algorithm based on three parameters: the number of SUHI-HSs, which the algorithm has to identify, and two threshold values as percentiles defining the minimum accepted value for a cell to be part of a SUHI-HS and the minimum average value for each SUHI-HS: for example, if the combination of the 95th and the 98th percentile thresholds is chosen, it means that each cell belonging to any SUHI-HS to be identified has a temperature higher or equal to the 95th percentile of the temperature range over the entire area of the city considered and the mean temperature of the entire SUHI-HS is equal to or higher than the 98th percentile. The percentile values are calculated based on the LST range for the entire analysis area selected by the users (e.g., the city, a neighbourhood etc.). For SUHI-HS detection, the algorithm starts by calculating the minimum acceptable values for a cell value and for an HS mean. With the two thresholds defined, each SUHI-HS identification is done step-by-step, starting with identifying the highest-temperature cell. Further, the algorithm searches all the neighbour cells to check if they meet the two threshold conditions. If checked, the cell is assigned to the current SUHI-HS and placed in a stack for its neighbours to be considered, too. If its neighbours do not meet the threshold conditions, they are dropped and not placed back in the stack. If the two conditions are not met, it will search in a different direction.

This process ensures that the expansion of an HS by grabbing appropriate neighbouring cells will eventually stop, completing the HS identification. The process will continue until no cell characterised by the two conditions is found in any direction. After the first SUHI-HS identification, the algorithm begins to search for the next SUHI-HS, considering all remaining cells that have not been assigned to the previously detected SUHI-HS(s) and keeping the same criteria/thresholds for identification. To identify each SUHI-HS, the stack's top value is extracted, and its neighbours are analysed.

Each cell assigned to an identified SUHI-HS will receive a unique HS identification number. This allows the detection order of HSs to be tracked and ranked and the already assigned cells to be registered. The analysis result is a raster layer where each cell has either a null value or an HS ID value. The script for the SUHI-HS detection (getHotSpots function) is developed in R and is freely available online at https://github.com/zsmagyari/SUHI. The results of the newly proposed method for SUHI-HS detection were compared with those obtained from the Getis-Ord Gi* statistics. In terms of the identified SUHI-HS locations, results returned by both methods are very similar (Fig. 2), thus validating the correctness of the algorithm we proposed.

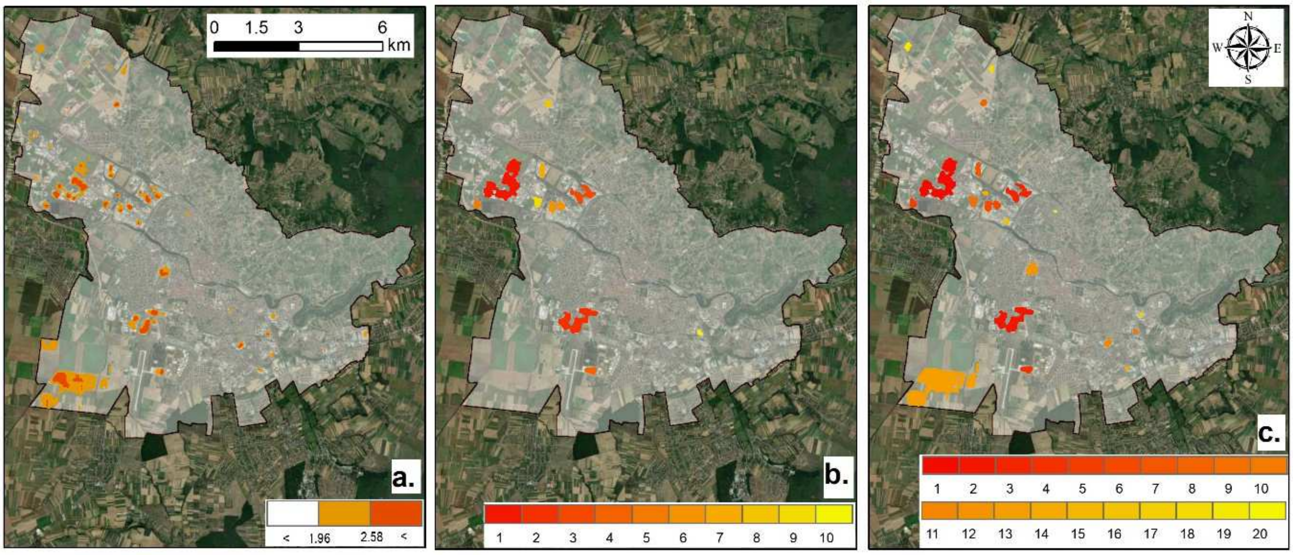

Fig. 2. SUHI-HS detection results using Getis-Ord Gi*: *(a) and the newly designed method in Oradea city (the most intense 10 (b) and 20 (c) SUHI-HSs with the 95th percentile as the minimum value for a cell and the 98th percentile average threshold of the entire HS values) derived from the Landsat image collected on 13 August 2023.*

However, the newly designed method gives the user more flexibility in choosing the intensity and expansion of the HSs. Similarly to SUHI-HS detection, a SUHI cool spot (SUHI-CS) detection algorithm was developed considering the lower percentile values as thresholds: e.g. if the pair of intensity thresholds of the 5th and the 2nd percentiles is selected, it means that each cell belonging to the SUHI-CS has a temperature lower or equal to the 5th percentile of the temperature range over the entire area of the city considered, and the entire SUHI-CS mean temperature is equal to or lower than the 2nd percentile of the entire analysis area.

3.2. SUHI-HSs severity detection

In addition to detecting the location and ranking of the SUHI-HSs on a single satellite image, the proposed method can quantify their severity by classes identified based on the combined assessment of their *persistence* and *overall intensity* derived from a multi-image analysis.

3.2.1. SUHI-HSs persistence assessment

The *persistence* of a SUHI-HS is calculated based on its frequency of occurrence on all satellite images available for a given period. When determining the SUHI-HS persistence, the sequence number obtained during the identification phase is not considered, as all are equally important.

The probability of a location (cell) being part of a SUHI-HS is calculated by summing up the cell values (0-not part of a SUHI-HS; 1-part of a SUHI-HS) for every location across different satellite images and normalising them by the total number of images. Thus, the method allows identifying areas where HSs consistently form, with persistence values ranging from 0 to 1, which are reclassified into a selectable number of classes. For example, we classified the persistence into three classes (1, 2, and 3), with class 1 including locations most frequently identified as part of SUHI-HSs derived from the entire satellite image set.

The functions for SUHI-HS persistence (hotspotPersistence) are freely available at https://github.com/zsmagyari/SUHI.

3.2.2. SUHI-HSs overall intensity assessment

The method/algorithm proposed allows the user to determine the *overall intensity* of SUHI-HSs by choosing the number of classes. Thus, to identify the overall intensity of a location (a cell in a SUHI-HS), it is necessary to define the number of SUHI-HSs to be considered for analysis and the number of intervals/classes into which they will be divided. Based on the number of intervals/classes, their boundaries are defined, and the algorithm will return the index of the interval in which a given location (cell) was most frequently found. As an example, we classified the Overall intensity into three classes (1, 2, and 3), with class 1 including locations most frequently identified as having high intensity derived from the entire satellite image set. It can be detected based on the hotspot Overall Intensity function. Similarly, functions can be used to evaluate the persistence and overall intensity of the SUHI-CSs by using the proper naming convention for input files (available at https://github.com/zsmagyari/SUHI).

3.2.3. SUHI-HSs severity assessment

The severity of the SUHI-HSs is detected by combining the two parameters detected (persistence and overall intensity) using a matrix combining the classes resulting from previous calculations. In the case study presented, from the persistence and overall intensity data, considering three classes for each feature, nine classes were derived (Fig. 3) to highlight areas representing the range from the most intense and highly persistent SUHI-HSs (the most severe SUHI-HSs) to that characterised by low occurrence and intensity (the lowest severe SUHI-HSs).

A similar analysis was conducted using the functions adjusted to detect persistence and overall intensity for the SUHI-CSs.

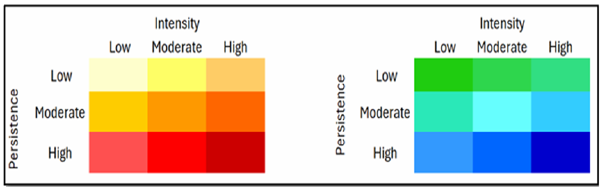

Fig. 3. The severity classes derived from persistence and overall intensity for SUHI-HSs (left) and SUHI-CSs (right).

Combined data on SUHI-HSs and SUHI-CSs can be represented on the same map using GIS, highlighting the most critical zones within the study area (SUHI-HSs), signalling the need for immediate administrative intervention, as well as the most comfortable ones (SUHI-CSs). Incorporating the imperviousness layer significantly increases the fragmentation of SUHI-HSs while reducing their size (Fig. 4).

SUHI-HS intensity, frequency, and severity can vary significantly within an urban landscape from one period to another, suggesting that more than a one-size-fits-all approach to urban planning and public health interventions may not be practical.

The proposed method addresses this challenge, allowing setting targeted/customized strategies to mitigate the adverse effects of each SUHI-HS. This approach enhances the efficiency of interventions and ensures that resources are allocated where they are most needed, maximising their impact. Compared to the Getis-Ord Gi* method, which is largely and the most frequently used for SUHI-HSs detection, the method we propose is more complex, allowing multi-image processing and providing additional SUHI-HS features: frequency, overall intensity, and severity.

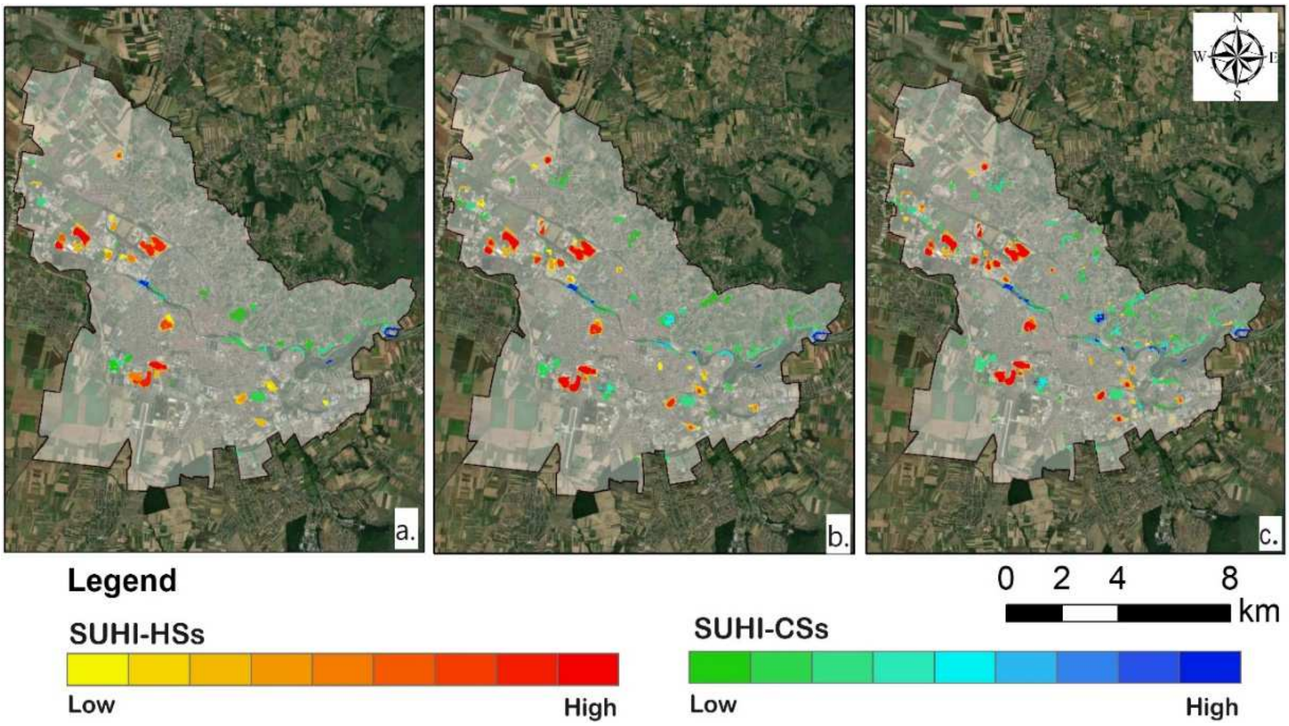

Fig. 4. SUHI-HSs and SUHI-CSs severity in Oradea city with various numbers of spots identified considering the impervious areas: *a) 10 spots; b) 20 spots; c) 50 spots*.

4. CONCLUSIONS

This research proposed an innovative SUHI-HSs detection method to comprehensively analyse the SUHI phenomenon, offering new insights into the spatial and temporal dynamics of heat distribution in urban areas. By employing a new algorithm developed in R, it can identify and rank the critical areas in terms of their persistence, intensity, and severity where heat systematically accumulates, thereby accentuating the risks associated with elevated temperatures. The method proposed has many advantages:

- it is easy to operate as the algorithms are developed in R, which is largely used by the scientific community;
- it allows the user to flexibly adjust the intensity thresholds and the number of spots identified according to local characteristics and planning purposes;
- it uses multi-image processing, providing a synthetic view, ranking the HSs over a longer period, based on their frequency, intensity, and severity, and allowing their prioritisation for interventions.

Beyond the state of the art, with its capability for single or multi-image processing to derive synthetic results and to rank the SUHI-HSs, the new method we propose could become a valuable tool not only for scientists in urban studies but also for city planners and decision-makers as it provides insights on the most critical locations that should be prioritised for urgent interventions in urban areas towards achievements of the various sustainable development goals (SDGs), such as SDG4 – Health and well-being; SDG7 – Affordable and clean energy; SDG9 – Industry, innovation and infrastructure; SDG11- Sustainable cities and communities; SDG13 – Climate action. Thus, the method can be used to identify critical areas for various types of interventions:

- modification of the urban landscape by replacing concrete/asphalt areas with new blue/green ones to diminish the intensity/severity of the SUHI-HS areas and increase the quality of life in the cities (SDG4, SDG9 and SDG11);
- transforming the SUHI-HSs generated by building roofs or parkings into non-SUHI-HS areas by covering them with solar panels (SDG7);
- identifying the best locations for first aid in case of extreme temperature events (e.g., heatwaves), which are severely amplified by the existence of the UHIs and their associated HSs (SDG4 and SDG13);
- identification of the urban tissue types that can generate SUHI-HSs, which should not be replicated when new build-up areas are designed (SDG9).

Additionally, the method has the advantage that it can be applied, not only in urban climate studies but in multiple domains and sectors where spatial data are available (*e.g.*, biodiversity).

5. ACKNOWLEDGEMENTS

This work was supported by a grant of the Ministry of Research, Innovation and Digitization, CCCDI - UEFISCDI, for the project Enhancing Quality of Life through Urban Heat Island Assessment -

INTEGRATE, project number PN-III-P2-2.1-PTE-2021-0147 (contract no. 70PTE/2022), within PNCDI III. The research is aligned with the PannEx RHP white book (www.pannex.org).

6. AUTHORS CONTRIBUTION

Conception and design: AEC – lead; ZMS - supporting; analysis and interpretation of the data: AEC and ZMS – lead; CH and SP - supporting; drafting of the paper: AEC and ZMS – leading; CH, SP – supporting; revising it critically for intellectual content: AEC – lead; ZMS - supporting, supervision: AEC. All authors approved the final version to be published and agreed to be accountable for all aspects of the work.

REFERENCES

Abera N., Yeshitela K. (2024), Exploring the thermal characteristics of different local climate zones in Addis Ababa, Ethiopia. Theoretical and Applied Climatology. DOI: https://doi.org/10.1007/s00704-024-04908-8

Abougendia S. M. (2023), Investigating surface UHI using local climate zones (LCZs), the case study of Cairo's River Islands. Alexandria Engineering Journal, 77, 293–307. DOI: https://doi.org/10.1016/j.aej.2023.06.071

Bruns J., Simko V. (2017), Stable Hotspot Analysis for Intra-Urban Heat Islands. GI_Forum, 1, 79–92. DOI: https://doi.org/10.1553/giscience2017_01_s79

Croitoru A. E., Magyari-Saska Z., Horvath C., Pop S. (2024), EGU General Assembly 2024. A New Method for Automatic Identification and Ranking the Urban Heat Island Hotspots. DOI: https://doi.org/10.5194/egusphere-egu24-11609

Cui F., Hamdi R., Yuan X., He H., Yang T., Kuang W., Termonia P., de Maeyer P. (2021), Quantifying the response of surface urban heat island to urban greening in global north megacities. Science of The Total Environment, 801, 149553. DOI: https://doi.org/10.1016/j.scitotenv.2021.149553

Deilami K., Kamruzzaman Md., Liu Y. (2018), Urban heat island effect: A systematic review of spatio-temporal factors, data, methods, and mitigation measures. International Journal of Applied Earth Observation and Geoinformation, 67, 30–42. DOI: https://doi.org/10.1016/j.jag.2017.12.009

Derdouri A., Wang R., Murayama Y., Osaragi T. (2021), Understanding the links between LULC changes and SUHI in cities: insights from two-decadal studies (2001–2020). Remote Sensing, 13, 3654. DOI: https://doi.org/10.3390/rs13183654

Echevarria Icaza L., van den Dobbelsteen A., van der Hoeven F. (2017), Using satellite imagery analysis to redesign provincial parks for a better cooling effect on cities: The case of South Holland. A+BE Architecture and the Built Environment, 7(20), 231–270. DOI: https://doi.org/10.7480/abe.2017.20.3478

European Environment Agency (2020), Imperviousness Density 2018 (raster 10 m and 100 m), Europe. In Database. DOI: https://doi.org/10.2909/3bf542bd-eebd-4d73-b53c-a0243f2ed862

Gartland L. M. (2012), Heat Islands. Routledge. DOI: https://doi.org/10.4324/9781849771559

Guerri G., Crisci A., Messeri A., Congedo L., Munafò M., Morabito M. (2021a), Thermal Summer Diurnal Hot-Spot Analysis: The Role of Local Urban Features Layers. Remote Sensing, 13(3), 538. DOI: https://doi.org/10.3390/rs13030538

Guerri G., Crisci A., Messeri A., Congedo L., Munafò M., Morabito M. (2021b), Thermal Summer Diurnal Hot-Spot Analysis: The Role of Local Urban Features Layers. Remote Sensing, 13(3), 538. DOI: https://doi.org/10.3390/rs13030538

Guha S. (2017), Dynamic analysis and ecological evaluation of urban heat islands in Raipur city, India. Journal of Applied Remote Sensing, 11(03), 1. DOI: https://doi.org/10.1117/1.JRS.11.036020

Hijmans R. J. (2023), Raster: Geographic Data Analysis and Modeling, R package version 3.6-24. URL: http://CRAN.R-project.org/package=raster

Ho H. C., Knudby A., Xu Y., Hodul M., Aminipouri M. (2016), A comparison of urban heat islands mapped using skin temperature, air temperature, and apparent temperature (Humidex), for the greater Vancouver area. Science of The Total Environment, 544, 929–938. DOI: https://doi.org/10.1016/j.scitotenv.2015.12.021

Houghton A., Prudent N., Scott J. E., Wade R., Luber G. (2012), Climate change-related vulnerabilities and local environmental public health tracking through GEMSS: A web-based visualization tool. Applied Geography, 33, 36–44. DOI: https://doi.org/10.1016/j.apgeog.2011.07.014

Hu L., Brunsell N. A. (2013), The impact of temporal aggregation of land surface temperature data for surface urban heat island (SUHI) monitoring. Remote Sensing of Environment, 134, 162–174. DOI: https://doi.org/10.1016/j.rse.2013.02.022

Ketterer C., Matzarakis A. (2016), Mapping the Physiologically Equivalent Temperature in urban areas using artificial neural network. Landscape and Urban Planning, 150, 1–9. DOI: https://doi.org/10.1016/j.landurbplan.2016.02.010

Krellenberg K., Link F., Welz J., Harris J., Barth K., Irarrazaval F. (2014), Supporting local adaptation: The contribution of socio-environmental fragmentation to urban vulnerability. Applied Geography, 55, 61–70. DOI: https://doi.org/10.1016/j.apgeog.2014.08.013

Magyari-Sáska Z. (2024), Ranked Surface Urban Heat Island detection for hotspots and cool spots. GitHub. URL: https://github.com/zsmagyari/SUHI. Accessed on May 3, 2024

Martin P., Baudouin Y., Gachon P. (2015), An alternative method to characterize the surface urban heat island. International Journal of Biometeorology, 59(7), 849–861. DOI: https://doi.org/10.1007/s00484-014-0902-9

Mathew A., Khandelwal S., Kaul N. (2016), Spatial and temporal variations of urban heat island effect and the effect of percentage impervious surface area and elevation on land surface temperature: Study of Chandigarh city, India. Sustainable Cities and Society, 26, 264–277. DOI: https://doi.org/10.1016/j.scs.2016.06.018

Qiao Q., Zhen Z., Lin Y. (2023), Assessment and simulation of thermal environments in Taiyuan urban built-up area, China. Frontiers in Ecology and Evolution, 11. DOI: https://doi.org/10.3389/fevo.2023.1261291

Santamouris M. (2020), Recent progress on urban overheating and heat island research. Integrated assessment of the energy, environmental, vulnerability and health impact. Synergies with the global climate change. Energy and Buildings, 207, 109482. DOI: https://doi.org/10.1016/j.enbuild.2019.109482

Sanyal J., Lu X. X. (2004), Application of remote sensing in flood management with special reference to monsoon Asia: a review. Natural Hazards, 33, 283–301. DOI: https://doi.org/10.1023/B:NHAZ.0000037035.65105.95

Shreevastava A., Bhalachandran S., McGrath G. S., Huber M., Rao P. S. C. (2019), Paradoxical impact of sprawling intra-Urban Heat Islets: Reducing mean surface temperatures while enhancing local extremes. Scientific Reports, 9(1), 19681. DOI: https://doi.org/10.1038/s41598-019-56091-w

Silva J. S., da Silva R. M., Santos C. A. G. (2018), Spatiotemporal impact of land use/land cover changes on urban heat islands: A case study of Paço do Lumiar, Brazil. Building and Environment, 136, 279–292. DOI: https://doi.org/10.1016/j.buildenv.2018.03.041

Sing Wong M., Peng F., Zou B., Shi W., Wilson G. J. (2016), Spatially Analyzing the Inequity of the Hong Kong Urban Heat Island by Socio-Demographic Characteristics. International Journal of Environmental Research and Public Health, 13. DOI: https://doi.org/10.3390/ijerph13030317

U. S. Geological Survey [USGS] (2024), Landsat 8 images. URL: www.usgs.gov. Accessed on February 10, 2024

Voogt J. A., Oke T. R. (2003), Thermal remote sensing of urban climates. Remote Sensing of Environment, 86, 370–384. DOI: https://doi.org/10.1016/S0034-4257(03)00079-8

Wang C., Chang H. T. (2020), Hotspots, Heat Vulnerability and Urban Heat Islands: An Interdisciplinary Review of Research Methodologies. Canadian Journal of Remote Sensing, 46(5), 532–551. DOI: https://doi.org/10.1080/07038992.2020.1816815

Wang J., Zhan Q., Guo H. (2015), The Morphology, Dynamics and Potential Hotspots of Land Surface Temperature at a Local Scale in Urban Areas. Remote Sensing, 8(1), 18. DOI: https://doi.org/10.3390/rs8010018

Yin C., Yuan M., Lu Y., Huang Y., Liu Y. (2018), Effects of urban form on the urban heat island effect based on spatial regression model. Science of The Total Environment, 634, 696–704. DOI: https://doi.org/10.1016/j.scitotenv.2018.03.350

Zhao X., Huang J., Ye H., Wang K., Qiu Q. (2010), Spatiotemporal changes of the urban heat island of a coastal city in the context of urbanisation. International Journal of Sustainable Development & World Ecology, 17(4), 311–316. DOI: https://doi.org/10.1080/13504509.2010.490333

Zhou Y., Zhao H., Mao S., Zhang G., Jin Y., Luo Y., Huo W., Pan Z., An P., Lun F. (2022), Exploring surface urban heat island (SUHI) intensity and its implications based on urban 3D neighborhood metrics: An investigation of 57 Chinese cities, Science of The Total Environment, Volume 847, https://doi.org/10.1016/j.scitotenv.2022.157662

Zhou Y., Smith S. J., Zhao K., Imhoff M., Thomson A., Bond-Lamberty B., Asrar G. R., Zhang X., He C., Elvidge C. D. (2015), A global map of urban extent from nightlights. Environmental Research Letters, 10, 054011. DOI: https://doi.org/10.1088/1748-9326/10/5/054011